THE JOURNAL OF BIOLOGICAL CHEMISTRY VOL. 289, NO. 47, pp. 32604–32616, November 21, 2014

Substrate Specificity of Human Protein Arginine Methyltransferase 7 (PRMT7)

*THE IMPORTANCE OF ACIDIC RESIDUES IN THE DOUBLE E LOOP**

Received for publication, September 6, 2014, and in revised form, October 6, 2014 Published, JBC Papers in Press, October 7, 2014, DOI 10.1074/jbc.M114.609271

You Feng, Andrea Hadjikyriacou, and Steven G. Clarke[1]

From the Department of Chemistry and Biochemistry and the Molecular Biology Institute, UCLA, Los Angeles, California 90095-1569

Background: Mammalian PRMT7 has been implicated in multiple biological processes, but its *in vivo* substrates have not been identified.
Results: Mutagenesis studies indicate key residues that affect the unique substrate preference of PRMT7.
Conclusion: Acidic residues within the double E loop confer specificity to PRMT7.
Significance: Understanding how PRMT7 recognizes its substrates will enhance our knowledge of its physiological role.

Protein arginine methyltransferase 7 (PRMT7) methylates arginine residues on various protein substrates and is involved in DNA transcription, RNA splicing, DNA repair, cell differentiation, and metastasis. The substrate sequences it recognizes *in vivo* and the enzymatic mechanism behind it, however, remain to be explored. Here we characterize methylation catalyzed by a bacterially expressed GST-tagged human PRMT7 fusion protein with a broad range of peptide and protein substrates. After confirming its type III activity generating only ω-N^G-monomethylarginine and its distinct substrate specificity for R*X*R motifs surrounded by basic residues, we performed site-directed mutagenesis studies on this enzyme, revealing that two acidic residues within the double E loop, Asp-147 and Glu-149, modulate the substrate preference. Furthermore, altering a single acidic residue, Glu-478, on the C-terminal domain to glutamine nearly abolished the activity of the enzyme. Additionally, we demonstrate that PRMT7 has unusual temperature dependence and salt tolerance. These results provide a biochemical foundation to understanding the broad biological functions of PRMT7 in health and disease.

Protein arginine methyltransferases (PRMTs)[2] are a family of enzymes that direct posttranslational methylation on targeted arginine residues in eukaryotes (1–4). Most mammalian PRMTs have been characterized as either type I enzymes that transfer up to two methyl groups from *S*-adenosyl-L-methionine (AdoMet) to the same terminal nitrogen atom forming ω-N^G-monomethylarginine (MMA) and ω-N^G,N^G-asymmetric dimethylarginine (ADMA) (PRMT1, -2, -3, -4, -6, and -8) or type II enzymes that transfer up to two methyl groups to different terminal nitrogen atoms, forming MMA and ω-N^G,N'^G-symmetric dimethylarginine (SDMA) (PRMT5) (1–4). However, PRMT7 has been found to produce MMA residues only, which defines it as the first type III PRMT (5–9). Recent work utilizing an insect cell-expressed mouse PRMT7 demonstrated a unique substrate specificity for R*X*R motifs among multiple basic residues (8). No other PRMT has been shown to have such narrow sequence specificity. These results led to the question of how the substrate selectivity of PRMT7 is restricted.

The human *PRMT7* gene encodes a protein containing ancestrally duplicated methyltransferase domains (1, 5). Although the advantage of duplicating the catalytic domain is unknown, it has been shown that deletion of either domain abolishes its activity (5). A number of studies have indicated that *PRMT7* expression in mammalian cells is regulated and can affect many biological processes, including pluripotency (10–12). Consistent with this role, *PRMT7* knockdown stimulates neuronal differentiation (13). Genetic variation of *PRMT7* may lead to increased sensitivity of cell lines to etoposide, a chemotherapeutic agent that targets topoisomerase II (14, 15). In addition, down-regulation of *PRMT7* sensitizes tumor cells to the topoisomerase I inhibitor camptothecin (16) and modulates cell response to DNA-damaging agents (17, 18). The role of PRMT7 has also been implicated in male germ line imprinting (19), Sm ribonucleoprotein methylation, and small nuclear ribonucleoprotein biogenesis (20) as well as breast cancer metastasis (21, 22). Thus, PRMT7 appears to participate in broad cellular processes under normal and disease conditions and is of therapeutic interest.

Given the extensive biological involvement of PRMT7, it is particularly important to get a clear understanding of its fundamental catalytic mechanism and cellular substrate specificity. Although the insect cell-expressed mouse PRMT7 showed higher catalytic activity than the bacterially expressed GST-

* This work was supported, in whole or in part, by National Institutes of Health Grant GM026020 (to S. G. C.) and GM007185, a Ruth L. Kirschstein National Research Service Award (to A. H.).
[1] To whom correspondence should be addressed: Dept. of Chemistry and Biochemistry and the Molecular Biology Institute, University of California, Los Angeles, 607 Charles E. Young Dr. E., Los Angeles, CA 90095-1569. Tel.: 310-825-8754; Fax: 310-825-1968; E-mail: clarke@mbi.ucla.edu.
[2] The abbreviations used are: PRMT, protein arginine methyltransferase; MMA, ω-N^G-monomethylarginine; [^{3}H]MMA, [*methyl*-^{3}H]ω-N^G-monomethylarginine; ADMA, ω-N^G,N^G-asymmetric dimethylarginine; SDMA, ω-N^G,N'^G-symmetric dimethylarginine; AdoMet, *S*-adenosyl-L-methionine; [^{3}H]AdoMet, *S*-adenosyl-[*methyl*-^{3}H]-L-methionine; [^{14}C]AdoMet, *S*-adenosyl-L-[*methyl*-^{14}C]methionine; GAR, glycine- and arginine-rich domain of human fibrillarin; TAT, trans-activator of transcription protein; RPL3, ribosomal protein L3; SmD3, small nuclear ribonucleoprotein D3; HBR, H2B repression domain; LDIG(69–72)AAAA, L69A/D70A/I71A/G72A mutant; LFD(145–147)WMG, L145W/F146M/D147G mutant; FD(146–147)LG, F146L/D147G mutant.

tagged human PRMT7 (7, 8), site-directed mutagenesis and protein expression and purification are facilitated in the bacterial system. In this work, we used the bacterial system to determine which residues of human PRMT7 are important for substrate recognition. We determined the substrate specificity with multiple peptide and protein substrates and then performed mutagenesis and kinetic analysis to probe the roles of specific residues of PRMT7 in the methylation reaction. We were able to demonstrate that two acidic residues within the catalytic double E loop are essential for its substrate specificity. Additionally, we revealed that mammalian PRMT7 is relatively tolerant to low temperature but is very sensitive to high temperature and salt. These findings will broaden our understanding of the reaction catalyzed by PRMT7 and set directions for future studies of its cellular functions.

EXPERIMENTAL PROCEDURES

Protein Expression and Purification—Human PRMT7 was subcloned into a pGEX-2T vector and expressed in *Escherichia coli* BL21 Star (DE3) cells (Invitrogen, C601003) as a GST fusion protein (7). The enzyme was purified using a glutathione-Sepharose affinity chromatography method modified from that described previously (7). Cells containing GST-PRMT7 plasmid were grown to an optical density at 600 nm of 0.6–0.8, and protein expression was induced with 0.4 mM isopropyl-D-thiogalactopyranoside at 16 °C overnight. The cells were lysed with sonication in a phosphate-buffered saline solution (137 mM NaCl, 2.7 mM KCl, 10 mM Na_2HPO_4, 2 mM KH_2PO_4, pH 7.4) containing 1 mM phenylmethylsulfonyl fluoride. The cell lysate was centrifuged for 50 min at 23,000 × *g* at 4 °C, and the supernatant containing GST-PRMT7 was loaded to glutathione-Sepharose 4B beads (Amersham Biosciences) according to the manufacturer's instructions. After washing with the phosphate-buffered saline solution, the bound protein was eluted with an elution buffer containing 30 mM glutathione, 50 mM HEPES, 120 mM NaCl, and 5% glycerol (pH 8.0). Glutathione in the eluted protein solution was reduced by 10–30-fold by adding fresh elution buffer without glutathione and reconcentrating using an Amicon centrifugation filter. Protein was quantified by a Lowry assay after trichloroacetic acid precipitation and stored at −80 °C as 50-μl aliquots. GST-GAR was expressed in *E. coli* BL21 Star (DE3) cells and purified with glutathione-Sepharose 4B affinity chromatography as described previously (7).

Mutagenesis—Primers for site-directed mutagenesis of GST-PRMT7 were synthesized by Integrated DNA Technologies (San Diego, CA). To create a catalytically inactive enzyme that cannot bind *S*-adenosylmethionine, quadruple mutations (L69A/D70A/I71A/G72A) were made using the forward primer 5′-GGACAGAAGGCCTTGGTTGCGGCCGCTGCGACTGGCACGGGACTC-3′ and the reverse primer 5′-GAGTCCCGTGCCAGTCGCAGCGGCCGCAACCAAGGCCTTCTGTCC-3′ (T_m = 89 °C). Other forward and reverse primers included 5′-GGTCACAGAGTTGTTTGGCACAGAGCTGATCGG-3′ and 5′-CCGATCAGCTCTGTGCCAAACAACTCTGTGACC-3′ (T_m = 80 °C) for D147G, 5′-CAGAGTTGTTTGACACAATGCTGATCGGGGAGGGGGC-3′ and 5′-GCCCCCTCCCCGATCAGCATTGTGTCAAACAACTCTG-3′ (T_m = 81 °C) for E149M, 5′-CCATCCACGTGCAGGAGAGCCTCGGAGAGCAGG-3′ and 5′-CCTGCTCTCCGAGGCTCTCCTGCACGTGGATGG-3′ (T_m = 79 °C) for T203E, 5′-CCACGTGCAGACCGAGCTCGGAGAGCAGGTCATCG-3′ and 5′-CGATGACCTGCTCTCCGAGCTCGGTCTGCACGTGG-3′ (T_m = 81 °C) for S204E, 5′-CTCTCCTCCTGGGCCAGCCGTTCTTCAC-3′ and 5′-GTGAAGAACGGCTGGCCCAGGAGGAGAG-3′ (T_m = 80 °C) for E478Q, 5′-AACATCCTGGTCACAGAGTGGATGGGCACAGAGCTGATCGGGGAG-3′ and 5′-CTCCCCGATCAGCTCTGTGCCCATCCACTCTGTGACCAGGATGTT-3′ (T_m = 78 °C) for triple mutation LFD(145–147)WMG, and 5′-CCTGGTCACAGAGTTGTTAGGCACAGAGCTGATCGG-3′ and 5′-CCGATCAGCTCTGTGCCTAACAACTCTGTGACCAGG-3′ (T_m = 89 °C) for the double mutation F146L/D147G. PCRs were set up according to the QuikChange Lightning site-directed mutagenesis kit (Agilent Technologies, Inc.), using 50 ng of the human PRMT7 pGEX-2T plasmid template, a 0.2 μM concentration of both primers, and 1 μl of QuikChange Lightning enzyme. The PCR was run at 95 °C for 2 min, followed by 18 cycles of reactions at 95 °C for 20 s, 60 °C for 10 s, and 68 °C for 4 min. There was an additional 5-min extension at 68 °C before the reaction was stopped at 4 °C. Amplification products were then digested using 2 μl of DpnI restriction enzyme for 5 min at 37 °C to remove the parental dsDNA. The mutant plasmid (3 μl) was then transformed into XL10-Gold ultracompetent *E. coli* cells, which were grown overnight at 37 °C on LB plates with ampicillin. Plasmid DNA from positive colonies was then sequenced on both strands to confirm the mutation (GeneWiz, Inc.). Mutant proteins, purified as described above, appeared to be folded correctly because their sensitivities to limited proteolysis were similar to the wild-type enzyme.

Peptide Substrates—Peptides H2B(23–37), H2B(23–37)R29K, H2B(23–37)R31K, H2B(23–37)R33K, H2B(23–37)R29K/R31K, H2B(23–37)R29K/R33K, H2B(23–37)R31K/R33K, H4(1–8), H4(14–22), H4(14–22)R17K, and H4(14–22)R19K were purchased from GenScript as HPLC-purified preparations with ≥90% purity. Peptides H4(1–21), H4(1–21)R3K, and H4(1–21)R3MMA were a kind gift from Drs. Heather Rust and Paul Thompson (Scripps Research Institute, Jupiter, FL) and were described previously (23, 24). P-SmD3 (a 28-residue fragment of pre-mRNA splicing protein SmD3) was a kind gift from Dr. Sidney Pestka (UMDNJ, Robert Wood Johnson Medical School, Piscataway, NJ) and was described previously (25). P-RPL3 (a 16-residue fragment of ribosomal protein L3) was purchased from Biosynthesis Inc. All peptides were verified by mass spectrometry with sequences listed in Table 1.

P81 Paper-based Methyl Transfer Assay—Enzymatic reactions contained 10–20 μM *S*-adenosyl-L-[*methyl*-^{14}C]methionine ([^{14}C]AdoMet; PerkinElmer Life Sciences; from a 425 μM stock (47 mCi/mmol) in 10 mM H_2SO_4/EtOH (9:1, v/v)) or 0.7 μM *S*-adenosyl-L-[*methyl*-^{3}H]methionine ([^{3}H]AdoMet; PerkinElmer Life Sciences; from a 7.0 μM stock (78.2 Ci/mmol) in 10 mM H_2SO_4/EtOH (9:1, v/v)), the indicated amounts of GST-PRMT7/mutant and peptide/protein substrate, and the indicated reaction buffer (typically 50 mM HEPES (pH 7.5), 10 mM NaCl, and 1 mM DTT) in a final reaction volume of 30 μl. After incubation, the reactions were quenched by loading 25 μl of the mixture onto a 2.5-cm diameter P81 phosphocellulose

ion exchange filter paper (Whatman), which was then washed three times at room temperature for 45 min in 300 ml of 0.05 M $NaHCO_3$ (pH 9). Positively charged peptides and proteins bind tightly to the phosphocellulose, whereas unreacted radioactive AdoMet washes off (26). After air drying at room temperature, the filters were submerged in 10 ml of Safety-Solve scintillation mixture (Research Products International, 111177) and subjected to liquid scintillation counting for three cycles of 3 min using a Beckman LS6500 instrument.

Amino Acid Analysis of Protein and Peptide Substrates by High Resolution Cation Exchange Chromatography—Substrates were methylated with the indicated amount of GST-PRMT7 wild-type or mutant protein and 0.7 μM [^{3}H]AdoMet in a final reaction volume of 60 μl. The reactions were incubated for 18–20 h at 23 °C in 50 mM potassium HEPES (pH 7.5), 10 mM NaCl, and 1 mM DTT. Control reactions were performed in the absence of substrate or enzyme or in the presence of the catalytically inactive enzyme mutant. When GST-GAR protein and P-SmD3 peptide were used as substrates, 60 μl of 25% (w/v) trichloroacetic acid with 20 μg of the carrier protein bovine serum albumin was added and incubated at 23 °C for 30 min prior to centrifugation at 4000 × *g* for an additional 30 min. The pellet was air-dried after washing with −20 °C acetone. When smaller peptides were used as substrates, 3–4 μl of 25% (w/v) trichloroacetic acid was used to lower the pH of the reaction mixture, and the peptides were isolated using OMIX C18 ZipTip® pipette tips (Agilent Technologies) followed by vacuum centrifugation to remove the elution buffer (trifluoroacetic acid/acetonitrile/H_2O (0.1:50:50)). Acid hydrolysis of all samples was performed *in vacuo* at 110 °C for 20 h with 50 μl of 6 N HCl. After removal of the HCl by vacuum centrifugation, samples were dissolved in 50 μl of water and mixed with 1 μmol each of ω-MMA (acetate salt; Sigma, M7033), SDMA (di-(*p*-hydroxyazobenzene)-*p*′-sulfonate salt; Sigma, D0390), and ADMA (hydrochloride salt; Sigma, D4268) as internal standards. High resolution cation exchange chromatography was then performed as described previously (8). The positions of the amino acid standards were determined using 570-nm absorbance after ninhydrin assay with 50 μl of column fractions (8). Radioactivity in 950 μl of each fraction was determined with liquid scintillation as described (8) but using the average of three 3-min counting cycles.

Fluorography of Methylated GST-GAR after SDS-PAGE—Methyl transfer reactions were set up with [^{3}H]AdoMet, GST-GAR, and GST-PRMT7 wild-type or mutant protein as described above for the amino acid analysis. For the time course, 10 μg of GST-GAR was preincubated at 23 °C for 5 h in the reaction buffer before the addition of the enzyme and [^{3}H]AdoMet. For the temperature dependence assays, reactions were set up using GST-GAR (10 μg, 4.8 μM final concentration), 0.8 μM GST-PRMT7, and 0.7 μM [^{3}H]AdoMet and were incubated for 16 h. In both cases, the reactions were quenched by the addition of SDS loading buffer and separated on 12.6% Tris-glycine gels, stained with Coomassie Blue for 1 h, destained overnight, treated in autoradiography-enhancing buffer (EN^{3}HANCE, PerkinElmer, 6NE9701) for 1 h and vacuum-dried. Dried gels were then exposed to autoradiography film (Denville Scientific Inc., E3012) for 3–4 days at −80 °C (Denville Scientific Inc., E3012). After exposure to film, ImageJ densitometric analysis was done on scanned images of the film and quantified as relative activity.

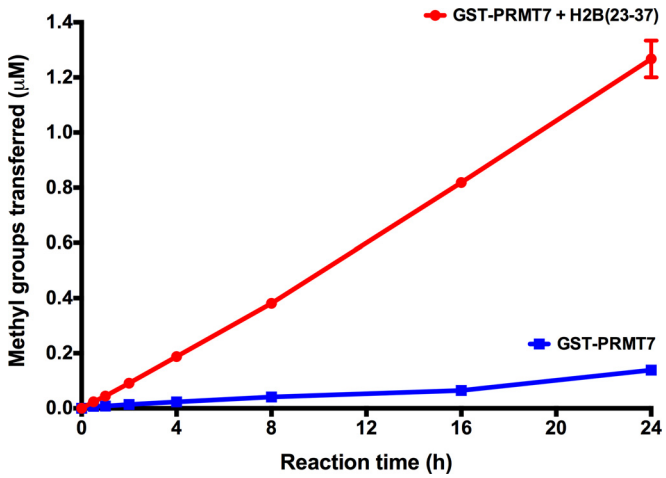

FIGURE 1. **Time course of the GST-PRMT7-catalyzed methylation reaction using the P81 paper assay.** Reactions were performed using 0.4 μM GST-PRMT7, 100 μM H2B(23–37) peptide, and 20 μM [^{14}C]AdoMet in a reaction buffer containing 50 mM potassium HEPES (pH 7.5), 10 mM NaCl, and 1 mM DTT in a total volume of 150 μl at 23 °C (*red points* and *line*). A control reaction was performed in the absence of the H2B(23–37) peptide substrate (*blue points* and *line*). At each time point, 20 μl of reaction mixture was spotted on a Whatman P81 filter, and the radioactive products were quantitated with liquid scintillation as described under "Experimental Procedures." Measurements were made in duplicate; when the range of values was larger than the plot symbol it is indicated with an *error bar*.

RESULTS

GST-PRMT7 Specifically Recognizes RXR Motifs Surrounded by Multiple Basic Residues in Peptide Sequences Based on Histone and Nonhistone Proteins—Full-length human PRMT7 was expressed and purified as a GST fusion protein from *E. coli* to avoid contamination from other PRMTs (27). Using a P81 filter paper assay as described under "Experimental Procedures," we optimized reaction conditions (temperature, pH, and salt) where product formation was linear over a 24-h period (Fig. 1). Importantly, at the 24 h point, only 6.3% of the initial AdoMet and only 1.3% of the initial peptide were converted to products, indicating that initial velocity conditions prevailed. To characterize the recognition sites for GST-PRMT7, methylation assays were first carried out with synthetic peptides containing the histone H2B repression domain (HBR, residues 27–34 (KKRKRSRK) (28)) that previously was observed to be methylated by insect cell-expressed PRMT7 (8). Peptides consisting of residues 23–37 were prepared with Arg-29, Arg-31, and Arg-33 as in the wild-type sequence or with one or two Arg → Lys substitutions at these sites (Table 1). The methylation products of these peptides were analyzed with high resolution amino acid analysis (Fig. 2). The wild-type peptide H2B(23–37) bearing the three arginines in the R*X*R*X*R sequence was well methylated by GST-PRMT7, producing only MMA (Fig. 2*A*). Peptides R29K and R33K, in which either the first or third arginine was mutated but where the R*X*R motif was retained remained good substrates with peak MMA radioactivity compared with the unmodified peptide of ~33 and ~6%, respectively (Fig. 2, *B* and *D*). However, peptide R31K with an R*XXX*R motif was rel-

TABLE 1

Peptide sequences

All arginine residues are highlighted in boldface type. Ac, acetyl.

Peptide	Sequence	Theoretical M_r	Observed M_r
H2B(23–37)	Ac-KKDGKK**R**K**R**S**R**KESY	1936.23	1935.60[a]
H2B(23–37)R29K	Ac-KKDGKKKK**R**S**R**KESY	1908.22	1908.00[a]
H2B(23–37)R31K	Ac-KKDGKK**R**KKS**R**KESY	1908.22	1907.80[a]
H2B(23–37)R33K	Ac-KKDGKK**R**K**R**SKKESY	1908.22	1908.00[a]
H2B(23–37)R29K/R31K	Ac-KKDGKKKKKS**R**KESY	1880.21	1879.60[a]
H2B(23–37)R29K/R33K	Ac-KKDGKKKK**R**SKKESY	1880.21	1879.60[a]
H2B(23–37)R31K/R33K	Ac-KKDGKK**R**KKSKKESY	1880.21	1879.60[a]
H4(1–21)	Ac-SG**R**GKGGKGLGKGGAK**R**H**R**KV	2133.47	2133[b]
H4(1–21)R3K	Ac-SGKGKGGKGLGKGGAK**R**H**R**KV	2105.46	2105[b]
H4(1–21)R3MMA	Ac-SG**R**(me)GKGGKGLGKGGAK**R**H**R**KV	2147.50	2147[b]
H4(1–8)	Ac-SG**R**GKGGK	787.87	787.60[a]
H4(14–22)	Ac-GAK**R**H**R**KVL	1106.33	1106.25[a]
H4(14–22)R17K	Ac-GAKKH**R**KVL	1078.32	1078.20[a]
H4(14–22)R19K	Ac-GAK**R**HKKVL	1078.32	1078.20[a]
H3(1–7)	Ac-A**R**TKQTA	816.91	816.50[a]
P-SmD3	AG**R**G**R**GKAAILKAQVAA**R**G**R**G**R**GMG**R**GN-amide	2792.25	2791[c]
P-RPL3	WGTKKLP**R**KTH**R**GL**R**K	1962.36	1961[c]
P-TAT	YG**R**KK**RR**Q**RRR**	1559.83	1559.60[a]
GAR (residues 1–148 of human fibrillarin)	MKPGFSP**R**GGGFGG**R**GGFGD**R**GG**R**GG**R**GGFGGG**R**G**R**GGGF**R**G**R**G**R**GGGGGGGGGGGGG **R**GGGGFHSGGN**R**G**R**G**R**GGK**R**GNQSGKNVMVEPH**R**HEGVFIC**R**GKEDALVTKNLVPG ESVYGEK**R**VSISEGDDKIEY**R**AWNPF**R**SKLAAAI	14,815	

[a] Data provided by GenScript Inc.
[b] Data from Refs. 23 and 24.
[c] Data from MALDI-TOF analysis.

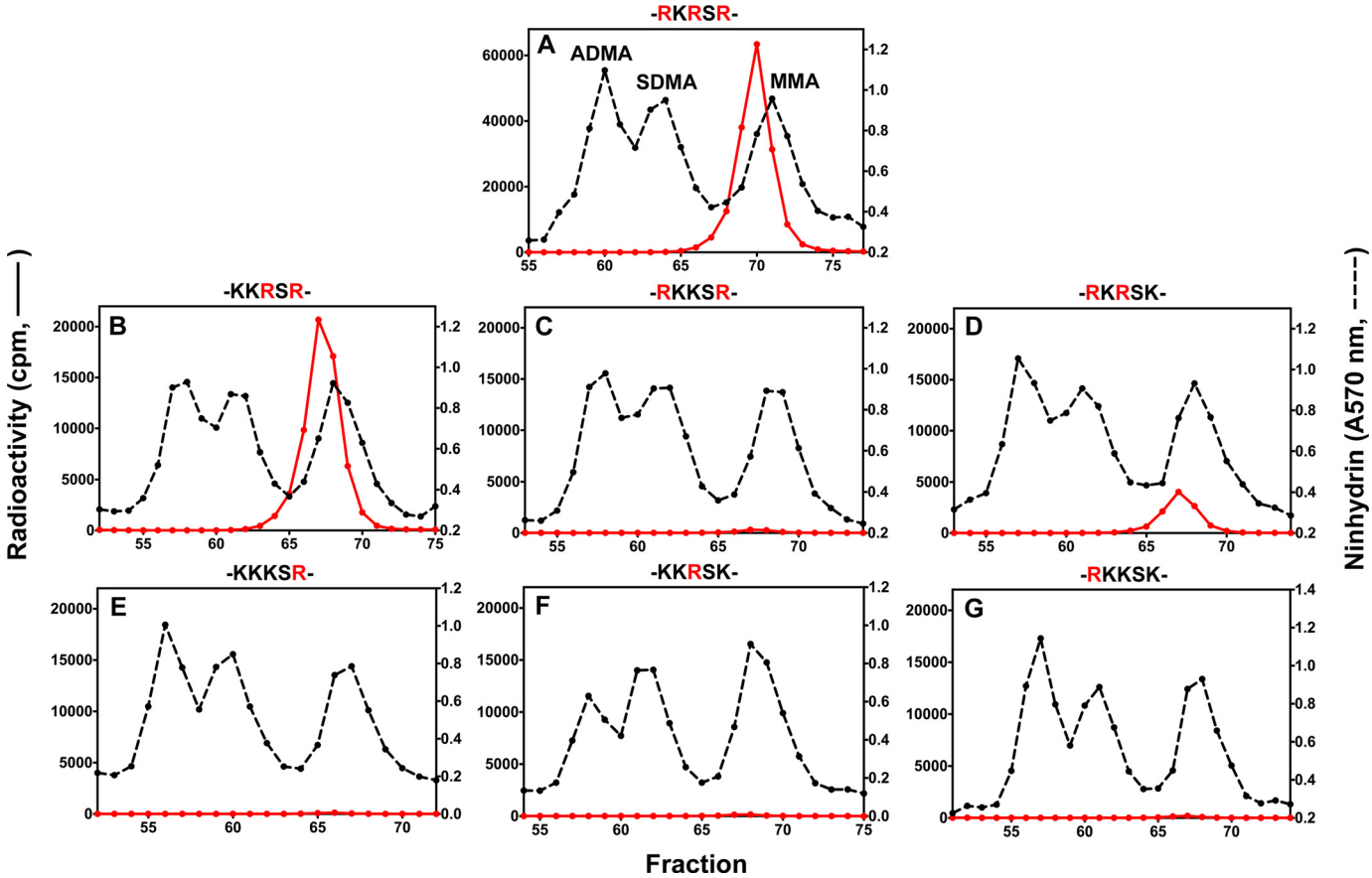

FIGURE 2. **Monomethylation of peptides derived from the DNA repression region of histone H2B by GST-PRMT7.** Peptides (12.5 μM; Table 1) were incubated with GST-PRMT7 (0.48 μM) and [^{3}H]AdoMet (0.7 μM) at 23 °C for 20 h as described under "Experimental Procedures." The reaction mixtures were then desalted with OMIX C18 ZipTip pipette tips, acid-hydrolyzed, and analyzed for methylated arginine species by amino acid analysis using high resolution cation exchange chromatography. The *red solid line* indicates the radioactivity of ^{3}H-methylated species; the *black dashed line* indicates the ninhydrin absorbance (570 nm) of ADMA, SDMA, and MMA standards. The ^{3}H-methyl derivatives of ADMA, SDMA, and MMA elute on this high resolution cation exchange column 1–2 min earlier than the non-labeled standards due to a tritium isotope effect (7, 8). *A–G*, PRMT7-catalyzed methylation products of H2B(23–37), H2B(23–37)R29K, H2B(23–37)R31K, H2B(23–37)R33K, H2B(23–37)R29K/R31K, H2B(23–37)R29K/R33K, and H2B(23–37)R31K/R33K, respectively. Partial sequences containing the target arginine sites (*highlighted* in *red*) are listed *above* the *panels*.

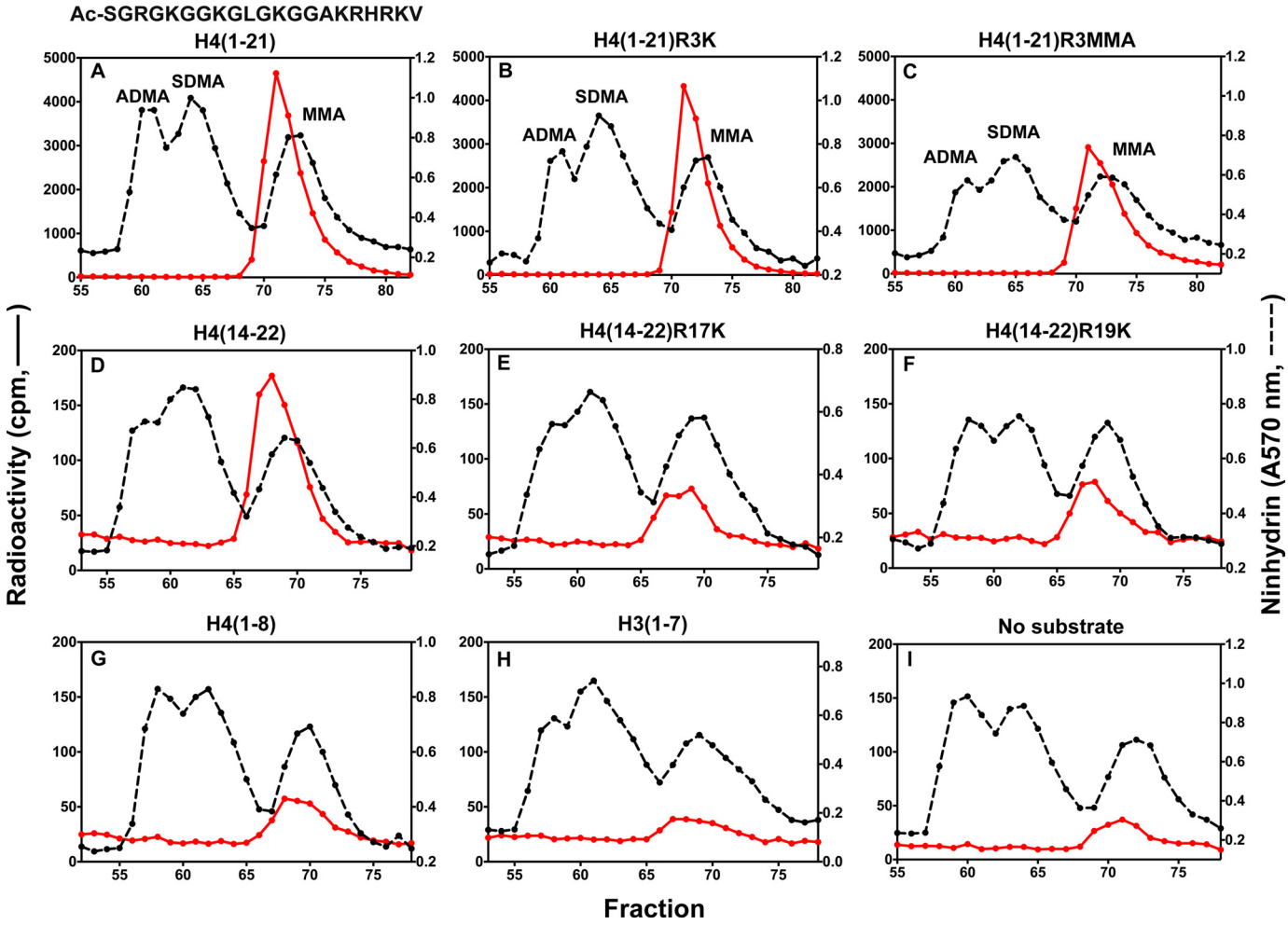

FIGURE 3. **Selective monomethylation in the RXR sequence of peptides derived from the N terminus of human histone H4.** Peptides (12.5 μM; Table 1) were incubated with [^{3}H]AdoMet (0.7 μM) and GST-PRMT7 (0.48 μM) at 23 °C for 20 h, as described under "Experimental Procedures." The reaction mixtures were desalted and tested by amino acid analysis, as described in the legend to Fig. 2. *A–C*, the GST-PRMT7-catalyzed methylation products of peptides H4(1–21), H4(1–21)R3K, and H4(1–21)R3MMA, respectively. The elution positions of the ADMA, SDMA, and MMA standards are indicated. *D–F*, GST-PRMT7-catalyzed methylation of peptides H4(14–22), H4(14–22)R17K, and H4(14–22)R19K. Control reactions with peptide H4(1–8), peptide H3(1–7), and no substrate (PRMT7 automethylation) are shown in *G–I*, respectively.

atively poorly methylated by GST-PRMT7, giving a peak radioactivity of only about 0.4% (Fig. 2*C*). Furthermore, when only a single arginine was present, as in peptides R29K/R31K, R29K/R33K, and R31K/R33K, less than 0.3% of the control radioactivity was seen (Fig. 2, *E–G*).

We also analyzed peptide substrates derived from the N-terminal 1–21, 1–8, or 14–22 residues of human histone H4 (Table 1). Peptide H4(1–21) was shown to be a good substrate for GST-PRMT7, with a single MMA peak (Fig. 3*A*). The replacement of Arg-3, the target site of PRMT1 and PRMT5 (23, 24, 26, 29–32), by either lysine or MMA in the peptide did not greatly decrease MMA formation or result in SDMA or ADMA formation (Fig. 3, *B* and *C*). Analysis of shorter peptides containing residues 14–22 of H4 and its R17K and/or R19K derivatives revealed that the loss of either the Arg-17 or Arg-19 residue markedly decreased MMA formation (Fig. 3, *D–F*). Finally, peptides containing residues 1–8 of H4 and residues 1–7 of H3 that lack the R*X*R motif were analyzed; little increase in MMA formation was seen over the small amount in the no-substrate control that reflects enzyme automethylation (Fig. 3, *G–I*). We did, however, find a role for the N-terminal residues in facilitating PRMT7-substrate interactions, because MMA formation in the H4(14–22) peptide was some 250-fold less than in the H4(1–21) peptide (Fig. 3, *A* and *D*).

We also searched for substrates for GST-PRMT7 with similar basic R*X*R motifs that were not derived from histones. Three peptides, P-TAT bearing a RKKRRQRRR sequence, P-SmD3 bearing RGRGK and RGRGR sequences, and P-RPL3 bearing a HRGLRK sequence, were analyzed (Table 1 and Fig. 4). Each of these peptides was recognized by GST-PRMT7 and only formed MMA. With P-TAT, the incorporation of ^{3}H-methyl groups approached the incorporation seen with the histone H2B(23–37) peptide (Fig. 2*A*), validating the preference of PRMT7 for the R*X*R motif in a high density of basic residues. P-SmD3 incorporated about 20% of the radioactivity seen with P-TAT, suggesting the importance of basic residues adjacent to the methylation sites. Finally, the P-RPL3 peptide only incorporated about 5% of the radioactivity of P-TAT. Here the insertion of a single residue between the pair of arginine residues appears to decrease PRMT7 recognition. Although we have not identified the precise sites of methylation in these peptides, all of them contain either R*X*R motifs or R*XX*R motifs in basic contexts.

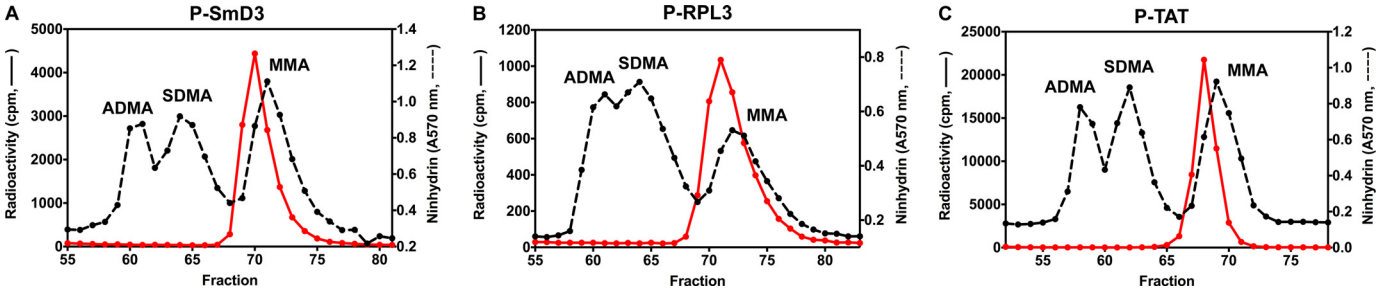

FIGURE 4. **Methylation of peptides derived from nonhistone substrates by GST-PRMT7.** Peptides (12.5 μM; Table 1) were methylated by GST-PRMT7 (0.48 μM) with [^{3}H]AdoMet (0.7 μM) at 23 °C for 18 h and detected by amino acid analysis as described in the legend to Fig. 2, except that trichloroacetic acid precipitation was used with the P-SmD3 substrate. *A–C*, PRMT7-catalyzed methylation products of peptides derived from SmD3, RPL3, and TAT proteins, respectively.

Taken together, the results shown in Figs. 2–4 suggest that bacterially expressed GST-human PRMT7 specifically recognizes pairs of arginine residues separated by one residue in a highly basic context to form only the monomethylated derivatives. This specificity is similar to that previously seen with the insect cell-expressed mouse PRMT7 enzyme (8).

Identification of Residues in PRMT7 Involved in Recognition of Basic RXR Substrates—Because the specific targeting of a basic R*X*R site by PRMT7 is unique among PRMT family members, we next tried to identify the residues in the enzyme important for substrate recognition. In all PRMT enzymes, the region following methyltransferase motif II has been associated with substrate binding (1, 2, 33) (Fig. 5). Here, PRMTs contain two highly conserved glutamate residues in a "double E" loop that directly bind the target arginine residue. We were intrigued to note that human PRMT7 has an aspartate residue (Asp-147) as the third residue following the initial glutamate in a position where all other PRMTs (except for PRMT9) contain a glycine residue. In addition, PRMT7 is the only human PRMT with an acidic residue (Glu-149) as the fifth residue following the initial glutamate of the double E loop. From the crystal structures of mouse and *Caenorhabditis elegans* PRMT7 (34, 35), Asp-147 and Glu-149 would be expected to face the substrate binding cavity. Interestingly, trypanosome PRMT7, which contains Gly and Met instead of Asp and Glu at these two positions (Fig. 5), methylates histone H4 at the non-R*X*R Arg-3 site, indicating that it may have a different substrate specificity from the human or mouse PRMT7 (9). However, it is clear that all of these species are type III PRMTs that only produce MMA as a product. We thus hypothesized that Asp-147 and Glu-149 might be important for targeting basic R*X*R sequences. Therefore, D147G and E149M mutations were made, changing the former into the conserved residue of the other PRMTs and the latter into the corresponding residue in TbPRMT7. We also constructed enzymes where residues 145–147 (LFD) in the double E loop of GST-PRMT7 were mutated to the conserved WMG sequence present in the type I PRMT1, -2, -3, -6, and -8 enzymes or mutated to the LLG sequence in the type II PRMT5 enzyme (Fig. 5). The C-terminal domain of human PRMT7 is not well conserved, with only one glutamate (Glu-478) present in the residues corresponding to the double E loop (Fig. 5, *red box*). To test the importance of this glutamate residue, a E478Q mutation was introduced. Finally, LC-MS/MS analysis on insect cell-expressed mouse PRMT7 (8) indicated possible phosphorylation sites on residues Thr-203 and Ser-204, which are conserved in human PRMT7. To determine whether these modifications might regulate the activity of the enzyme, T203E and S203E mutations were made to mimic the phosphorylated Thr-203 and Ser-204 residues.

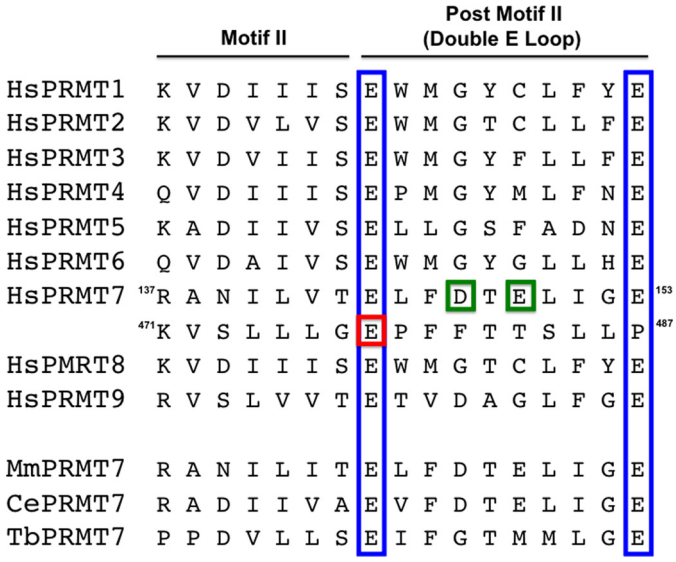

FIGURE 5. **Sequence alignment of the substrate binding motif II and post-motif II (double E loop) of PRMTs.** The two catalytic glutamate residues on the double E loop are *highlighted* with *blue boxes*. Two additional acidic residues (Asp-147 and Glu-149) in the N-terminal domain post-motif II in HsPRMT7 are *highlighted* with *green boxes*. The only acidic residue (Glu-478) on the C-terminal domain post-motif II in HsPRMT7 is *highlighted* with a *red box*. *Hs*, *Homo sapiens*; *Mm*, *Mus musculus*; *Ce*, *C. elegans*; *Tb*, *Trypanosoma brucei*; *HsPRMT9*, the gene product on human chromosome 4q31.

Amino acid analysis was carried out on all of the GST-PRMT7 mutants with the H2B(23–37) peptide as a substrate. As indicated in Fig. 6, all the mutations lowered the methyl group incorporation in H2B(23–37) to different levels compared with the wild-type enzyme (Fig. 6*H*), although none of them altered the type III methyltransferase activity because only MMA product was observed. The radioactivity in MMA generated by GST-D147G and GST-E149M with the peptide (Fig. 6, *A* and *B*) was ~6 and ~17% of that by the wild-type enzyme, respectively. However, the enzyme automethylation in these mutants in the absence of peptide was 4- and 3-fold higher when compared with that of the wild type (Fig. 6*H*, *blue line*). Thus, these two mutants were more active with auto-

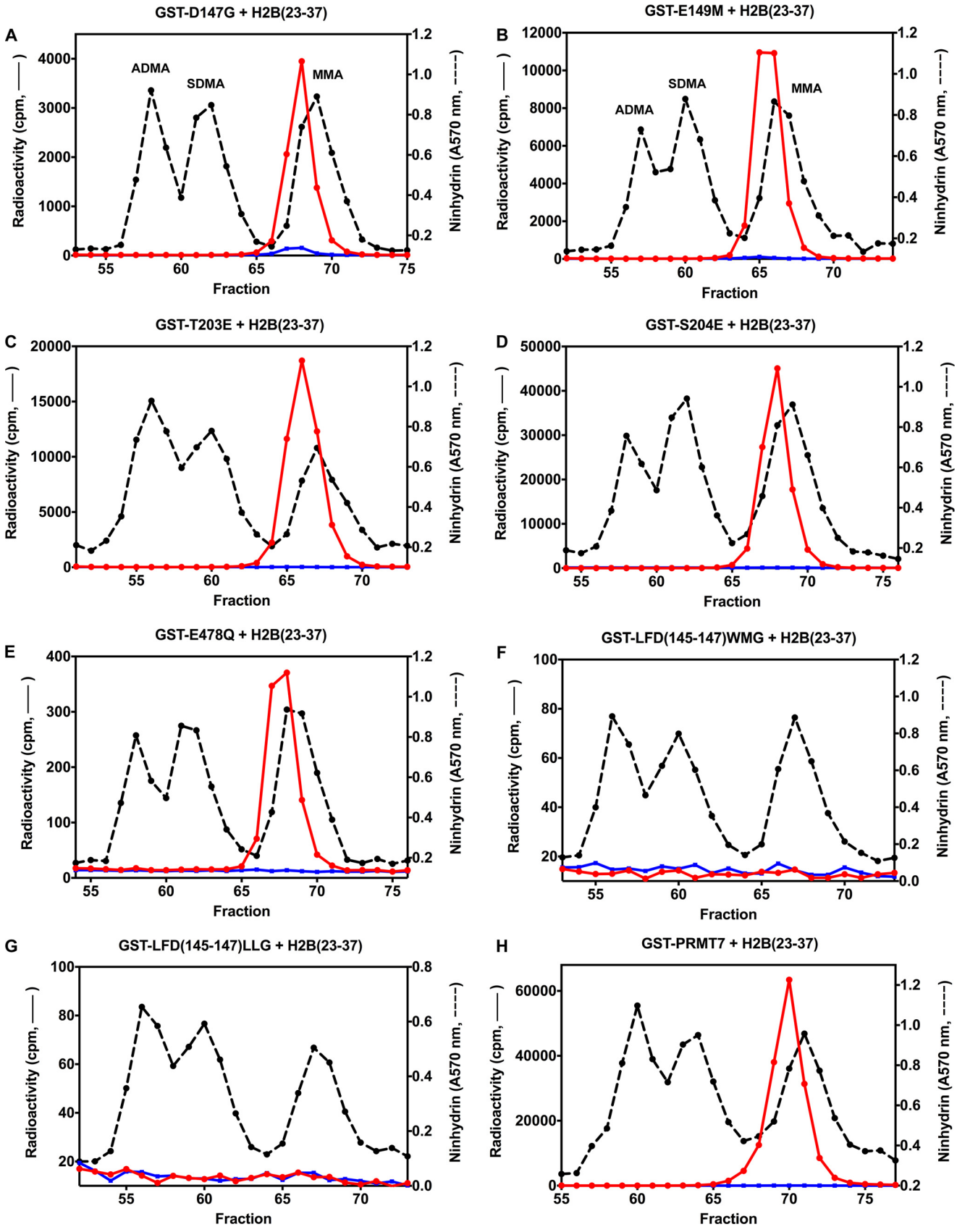
A
GST-D147G + H2B(23-37)
ADMA
SDMA
MMA
B
GST-E149M + H2B(23-37)
ADMA
SDMA
MMA
C
GST-T203E + H2B(23-37)
D
GST-S204E + H2B(23-37)
E
GST-E478Q + H2B(23-37)
F
GST-LFD(145-147)WMG + H2B(23-37)
G
GST-LFD(145-147)LLG + H2B(23-37)
H
GST-PRMT7 + H2B(23-37)
Radioactivity (cpm, ——)
Ninhydrin (A570 nm, ----)
Fraction

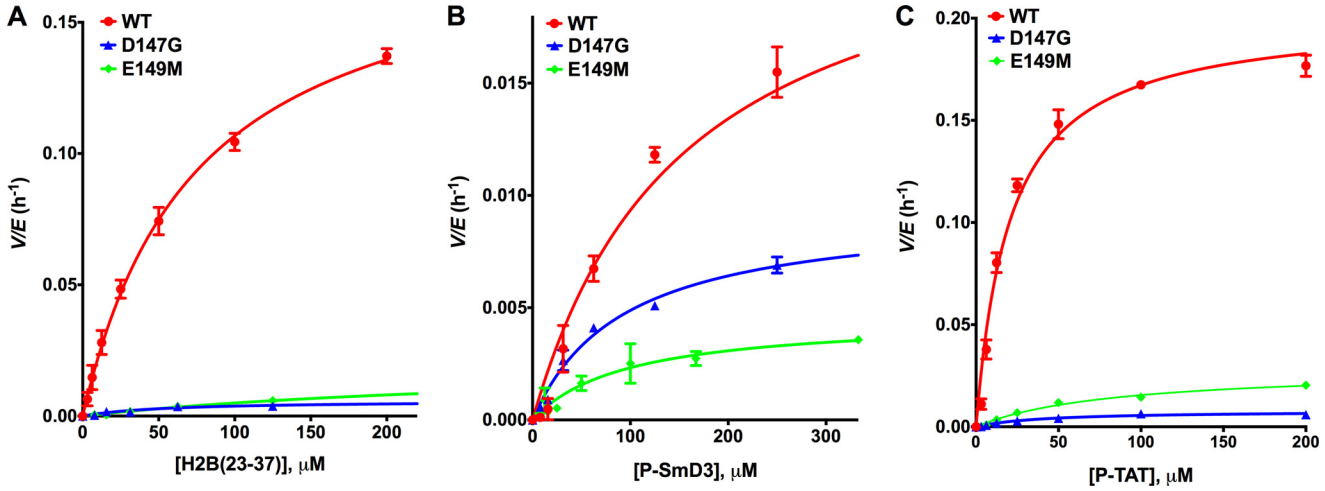

FIGURE 7. **Michaelis-Menten analyses for GST-PRMT7 mutants with H2B(23–37) (*A*), P-SmD3 (*B*), and P-TAT (*C*) as substrates.** Kinetic initial rate measurements were taken, and data were fit to the Michaelis-Menten equation as described in the legend to Table 2. Each assay was performed in duplicate, and the *error bars* indicate the range. The *solid lines* represent the curves from the fitted k_{cat} and K_m values shown in Table 2. Data are shown for the wild-type enzyme (*red*), the D147G mutant (*blue*), and the E149M mutant (*green*).

methylation but less active with the H2B(23–37) peptide containing the HBR domain, giving a clue that Asp-147 and Glu-149 might be essential in regulating the substrate specificity. Although the T203E and T204E mutants showed similar levels of product accumulation to the wild-type enzyme (Fig. 6, *C* and *D*), the E478Q mutant surprisingly displayed only <1% of radioactivity incorporation to H2B(23–37) (Fig. 6*E*), demonstrating the importance of the acidic residue Glu-478 in the region corresponding to the double E loop in the C-terminal domain. Little or no activity was observed for the LFD(145–147)WMG and the FD(146–147)LG mutants designed to mimic the double E loops of the type I and type II enzymes, respectively (Figs. 5 and 6 (*F* and *G*)).

Substrate Specificity Changes Determined by Kinetic Analysis of GST-PRMT7 Mutants with Peptide Substrates—We then performed detailed kinetic characterization on the wild-type GST-PRMT7 and mutants GST-D147G, GST-E149M, and GST-S204E using different peptide substrates. Under our conditions, product formation catalyzed by GST-PRMT7 is linear for 24 h at 23 °C (Fig. 1). In these experiments, we incubated the reactions for 5 h, a time at which substrate consumption would be expected to be less than 2%. The concentration of peptide substrate was varied, whereas the [^{14}C]AdoMet was fixed at 15 μM for the kinetic analyses. As shown in Fig. 7, the Michaelis-Menten curves showed similar patterns for H2B(23–37) and P-TAT, which both contain very basic R*X*R target sites. The D147G and E149M mutants showed very little activity toward these two peptides compared with the wild type. However, the catalytic pattern of the wild-type and mutant enzymes for the P-SmD3 substrate containing the less basic RGRG repeats was distinct. Although the P-SmD3 peptide was a markedly poorer substrate than H2B(23–37) and P-TAT, the relative activities of the D147G and E149M mutations were much greater with the P-SmD3 substrate. These results suggest that Asp-147 and Glu-149 are particularly important in recognizing the basic residues surrounding the target site. Interestingly, the activity of the E149M enzyme was greater than that of the D147G enzyme with the more basic H2B(23–37) and P-TAT substrates but lower with the less basic P-SmD3 substrate. The k_{cat} and K_m values for all of the mutants tested are shown in Table 2, where the k_{cat}/K_m value best reflects the overall substrate specificity. Compared with wild-type GST-PRMT7, the k_{cat}/K_m values are 23- and 38-fold lower for GST-D147G and GST-E149M in

TABLE 2

Kinetic data for selected GST-PRMT7 mutants with different substrates

P81 paper assays were performed with varying concentrations of each substrate (typically 0–200 μM) incubated with 15 μM [^{14}C]AdoMet and 0.5 or 0.75 μM GST-PRMT7 or its mutant in the reaction buffer (50 mM potassium HEPES (pH 7.5), 10 mM NaCl, and 1 mM DTT) in a total volume of 30 μl at 23 °C. After 5 h, 25 μl of the reaction mixture was spotted onto the P81 filter paper, which was washed and dried as described under "Experimental Procedures." The radioactivity on the P81 paper was detected by liquid scintillation as described. The initial velocity as a function of substrate concentration was fit to the Michaelis-Menten equation with the Prism 6 program, which gave the k_{cat} and K_m and their S.E. values as shown below.

Enzyme	Substrate	k_{cat}	K_m	k_{cat}/K_m
		$\times 10^{-3}\ h^{-1}$	μM	$\times 10^{-4}\ \mu M^{-1}\ h^{-1}$
GST-PRMT7	H2B (23–37)	186 ± 6	75 ± 5	25 ± 2
	P-SmD3	24 ± 2	155 ± 27	1.6 ± 0.3
	P-TAT	201 ± 7	21 ± 2	98 ± 11
GST-D147G	H2B (23–37)	5.9 ± 0.5	55 ± 15	1.1 ± 0.3
	P-SmD3	9.4 ± 0.4	92 ± 12	1.0 ± 0.1
	P-TAT	7.9 ± 0.7	42 ± 10	1.9 ± 0.5
GST-E149M	H2B (23–37)	21 ± 1	325 ± 36	0.65 ± 0.08
	P-SmD3	4.6 ± 0.6	96 ± 29	0.48 ± 0.16
	P-TAT	29 ± 2	84 ± 12	3.5 ± 0.5
GST-S204E	H2B (23–37)	85 ± 5	63 ± 8	13 ± 2
	P-SmD3	7.5 ± 0.6	26 ± 7	2.9 ± 0.8
	P-TAT	81 ± 1	7.7 ± 0.6	110 ± 8

FIGURE 6. **Methylated product analyses of PRMT7 mutants with the H2B(23–37) peptide as a substrate.** Peptide (12.5 μM) was methylated by a 0.48 μM concentration of the indicated GST-PRMT7 mutant (*A–G*) with [^{3}H]AdoMet (0.7 μM) in a 60-μl reaction for 18 h. The products were acid-hydrolyzed and subjected to cation exchange coupled with amino acid analysis as described in the legend to Fig. 2. The *red line* shows radioactivity with the full reaction mixture; the *blue line* shows the radioactivity in enzyme automethylation (no H2B(23–37) was present). For ease of comparison, the data for wild-type GST-PRMT7 (*H*) are combined from the data shown in Fig. 2*A* and Fig. 3*I*. In *H*, the reaction was incubated for 20 h but under conditions otherwise identical to those shown in *A–G*, where the incubation was 18 h.

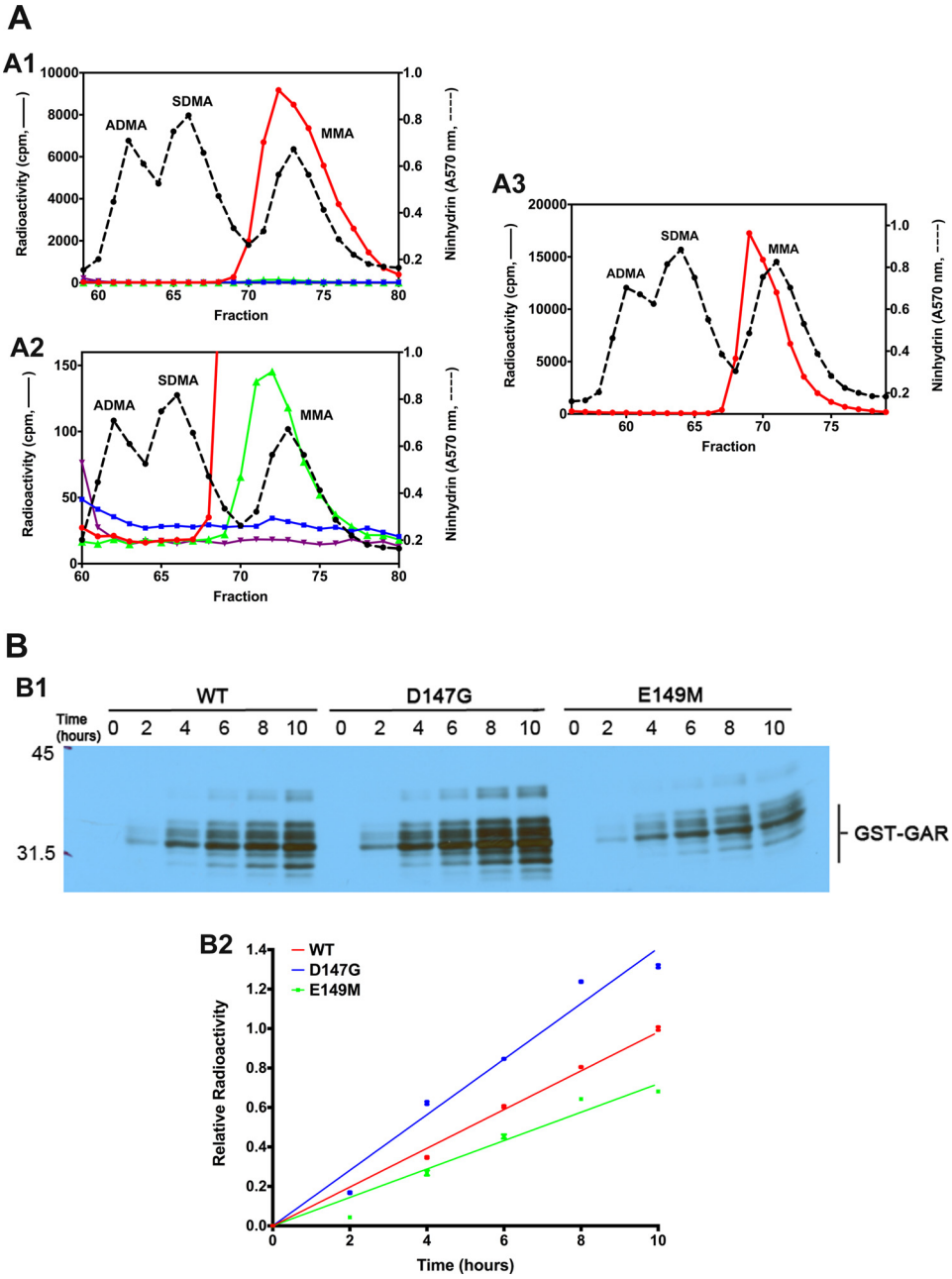

FIGURE 8. **Methylation of the GST-GAR protein by GST-PRMT7 and its mutants.** *A*, GST-PRMT7-catalyzed formation of MMA on GST-GAR. *A1*, *in vitro* methylation reactions were performed as described in the legend to Fig. 2 using 6 μg of GST-GAR (2.9 μM) and 3 μg of wild-type GST-PRMT7 or mutant LDIG(69–72)AAAA (0.48 μM). The reactions were allowed to proceed at 23 °C for 20 h before quenching by trichloroacetic acid precipitation. Incubations in the absence of GST-PRMT7 or GST-GAR were used as controls. After acid hydrolysis, the methylated amino acid derivatives were analyzed by high resolution cation exchange chromatography together with standards of ADMA, SDMA, and MMA as described under "Experimental Procedures." ^{3}H radioactivity (*solid lines*) and ninhydrin absorbance of the methylated arginine standards (*dashed lines*; elution positions indicated) were detected with liquid scintillation counting and 570-nm absorbance, respectively. *Red*, wild-type GST-PRMT7 with GST-GAR; *green*, wild-type GST-PRMT7 alone; *blue*, LDIG(69–72)AAAA mutant enzyme with GST-GAR; *purple*, GST-GAR alone. *A2*, magnification of the radioactivity scale to show PRMT7 automethylation (*green*), the residual activity of LDIG(69–72)AAAA (*blue*), and the absence of ADMA and SDMA in the reaction products (*red*). *A3*, premethylated GST-GAR generates only MMA in a PRMT7-catalyzed reaction. GST-GAR (6 μg) was preincubated with unlabeled AdoMet (125 μM final) and GST-PRMT7 (3 μg) in 40 μl of reaction buffer at 23 °C for 24 h to enrich for MMA. Next, the unlabeled AdoMet concentration was lowered to 0.05 μM by adding fresh reaction buffer, and the sample was concentrated using an Amicon Ultra centrifugal filter (Millipore). Then [^{3}H]AdoMet (0.7 μM) and extra GST-PRMT7 (2.4 μg) were added into the reaction mixture, which was incubated at 23 °C for another 20 h before acid hydrolysis and cation exchange chromatography. The radioactivity of ^{3}H-labeled protein residue was plotted in comparison with the standards. *B*, time course of GST-GAR methylation by double E loop GST-PRMT7 mutants. *B1*, fluorography of ^{3}H-methylated GST-GAR after reaction with wild type or mutant GST-PRMT7 as described under "Experimental Procedures." Dried gels were exposed to autoradiography film for 4 days at −80 °C. Reactions were run in duplicate on separate gels, one of which is shown here. *B2*, quantification of GST-GAR methylation catalyzed by wild type GST-PRMT7 (*red*), D147G (*blue*), and E149M (*green*). Data were acquired from the densitometric analysis of the autoradiography film and are shown as activity relative to that at the 10-h time point for the wild-type enzyme. *Error bars*, range of duplicate experiments.

methylating H2B(23–37) and 52- and 28-fold lower for these two mutants in methylating P-TAT, whereas they are only 2- and 3-fold lower for them in methylating P-SmD3. These data indicate that Asp-147 and Glu-149 are responsible for the selectivity of PRMT7 for R*X*R residues in basic sequence contexts. Looking at the H2B(23–37) substrate only, GST-D147G

showed a 32-fold smaller k_{cat} and a similar K_m compared with the wild type, indicating that Asp-147 in the double E loop is mainly involved in catalysis; GST-E149M showed a 9-fold smaller k_{cat} and a 4-fold larger K_m compared with the wild type, indicating that Glu-149 in the double E loop is involved in both catalysis and substrate binding. As for GST-S204E, the k_{cat}/K_m values for all three substrates are generally similar to the wild type because the k_{cat} and K_m for individual peptide are both decreased. It is possible that the potential phosphorylation on Ser-204 might increase the substrate binding affinity.

Specificity of GST-PRMT7 Mutants for the Protein Substrate GST-GAR—To confirm the alteration of substrate specificity for the GST-D147G and GST-E149M PRMT7 mutant enzymes, we also analyzed the substrate GST-GAR, consisting of residues 1–148 of human fibrillarin (7, 36) and containing similar RGRG repeats as in the P-SmD3 peptide (Table 1). We first performed amino acid analysis on the reaction products. Fig. 8*A* shows that wild-type GST-PRMT7 generated only [^{3}H]MMA on GST-GAR (Fig. 8*A1*). A small amount of [^{3}H]MMA automethylation was found for the enzyme-alone control (about 1.4% of that with GST-GAR) (Fig. 8*A2*, *green line*); less than 0.1% of [^{3}H]MMA was detected with the AdoMet binding-deficient mutant enzyme GST-LDIG(69–72)AAAA and GST-GAR (Fig. 8*A2*, *blue line*). In addition, to verify if PRMT7 adds a second methyl group to monomethylated arginine residues, GST-GAR was premethylated with unlabeled AdoMet to enrich for MMA, and then [^{3}H]AdoMet was added for detection of methylated product. Again, only the [^{3}H]MMA peak was observed with no detectable [^{3}H]SDMA or [^{3}H]ADMA formation (Fig. 8*A3*). These results confirm that GST-PRMT7 is unable to transfer a second methyl group to the arginine site where one methyl group is already present.

Next, SDS-PAGE and fluorography were performed to monitor the time courses of GST-GAR methylation catalyzed by wild-type GST-PRMT7 and mutants GST-D147G and GST-E149M (Fig. 8*B*). The density of methylated GST-GAR bands on the fluoroimage (Fig. 8*B1*) was quantified, and product formation indicated by the relative radioactivity was linear for up to 10 h with the wild-type and mutant enzymes (Fig. 8*B2*). Importantly, the activities of the mutant enzymes were similar to that of the wild-type enzyme; GST-D147G showed, in fact, a higher catalytic activity. These results stand in marked contrast to those obtained above with the H2B(23–37) and P-TAT peptides, where very little activity was seen in the mutants compared with the wild type (Fig. 7, *A* and *C*). Therefore, the substrate specificity change is confirmed here: mutation of Asp-147 and Glu-149 on the double E loop does not greatly affect the specificity of PRMT7 for RGRG-containing GST-GAR but dramatically decreases its selectivity for substrates rich in basic residues.

Unusual Dependence of PRMT7 Activity on Temperature and Salt Concentration—During the reaction condition optimization, we found that PRMT7 had an unusual temperature dependence. When we tested the temperature effect on bacterially expressed human GST-PRMT7 with H2B(23–37) as a substrate in the P81 paper assay (Fig. 9*A*), the peak activity was found between 15 and 25 °C. The enzyme remained ~50% active when the temperature was lowered to 5 °C, whereas its

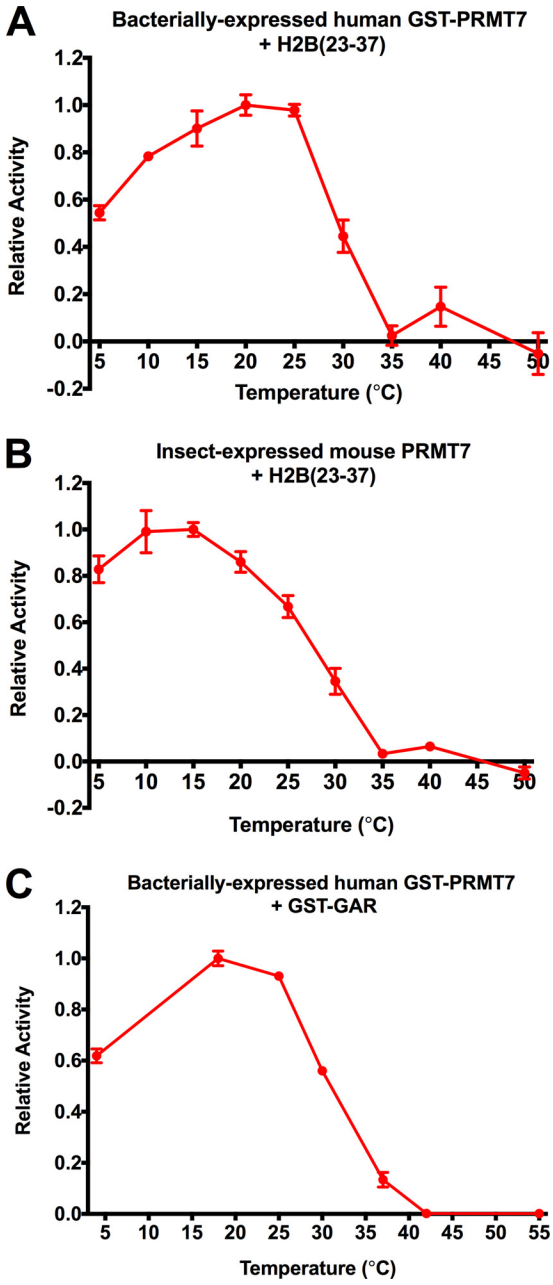

FIGURE 9. **Effect of temperature on PRMT7 activity.** *A*, temperature dependence of bacterially expressed human GST-PRMT7 with the H2B(23–37) peptide as a substrate. The reactions contained 0.4 μM GST-PRMT7, 40 μM H2B(23–37), and 10 μM [^{14}C]AdoMet in a 30-μl reaction buffer of 50 mM potassium HEPES (pH 7.5), 10 mM NaCl, and 1 mM DTT. The reactions were incubated at the indicated temperature for 16 h. After incubation, the reaction mixtures were spotted on Whatman P81 filter paper and washed, and the radioactivity in the protein products was determined by liquid scintillation counting, as described under "Experimental Procedures." The reaction background (radioactivity in the absence of enzyme) was subtracted, and the relative activity is shown in comparison with the activity at 20 °C. *B*, temperature dependence of insect cell-expressed mouse PRMT7 with the H2B(23–37) peptide as a substrate. The reactions contained 0.1 μM PRMT7, 10 μM H2B(23–37), and 10 μM [^{14}C]AdoMet in 50 mM potassium HEPES (pH 7.5), 10 mM NaCl, and 1 mM DTT and were analyzed as in *A*, except that the relative activity is shown in comparison with the value at 15 °C. *C*, temperature dependence of bacterially expressed human GST-PRMT7 with GST-GAR as a substrate. 4.8 μM GST-GAR, 0.8 μM GST-PRMT7, and 0.7 μM [^{3}H]AdoMet were incubated in the reaction buffer for 16 h. The methylated products were separated with 12.6% SDS-PAGE, treated with EN^{3}HANCE buffer, vacuum-dried, and exposed to autoradiography film for 3 days at −80 °C. Densitometric analysis was done on scanned images of the film, and quantification of the data is shown as activity relative to that at 18 °C. In each case, the assays were done in duplicate, and the *error bars* show the range of the data.

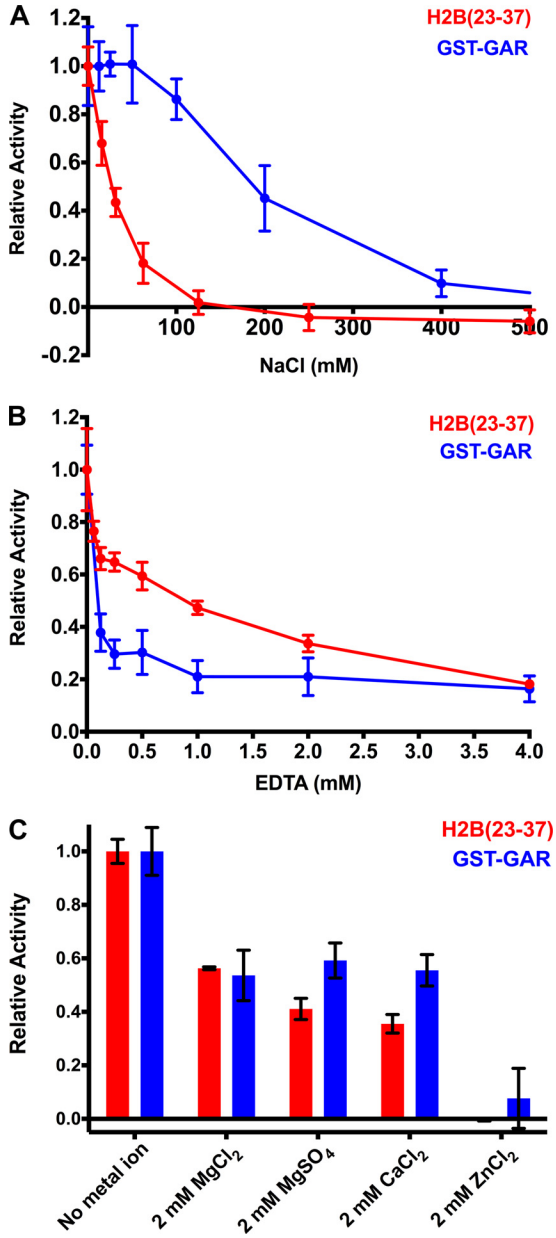

FIGURE 10. **Effect of NaCl, EDTA, and metal ions on PRMT7 activity.** A, salt effect. The reaction buffer contained 50 mM potassium HEPES (pH 7.5), 1 mM DTT, and different concentrations of NaCl. When H2B(23–37) peptide was used as a substrate (*red*), 20 μM peptide, 0.4 μM GST-PRMT7, and 10 μM [^{14}C]AdoMet were incubated for 16 h at 23 °C. When GST-GAR was used as a substrate (*blue*), 2 μg of GST-GAR, 0.8 μg of GST-PRMT7, and 0.7 μM [^{3}H]AdoMet were incubated for 18 h at 23 °C. The reaction mixtures were then spotted on Whatman P81 filter paper and washed, and the radioactivity in the methylated products was determined by liquid scintillation as described under "Experimental Procedures." Radioactivity in controls lacking enzyme (peptide assay) or enzyme and substrate (protein assay) were subtracted. *B*, EDTA effect. The reaction buffer contained 50 mM potassium HEPES (pH 7.5), 10 mM NaCl, 1 mM DTT, and different concentrations of EDTA. When H2B(23–37) was used as a substrate (*red*), 40 μM H2B(23–37), 0.4 μM GST-PRMT7, and 10 μM [^{14}C]AdoMet were incubated at 23 °C for 16.5 h. When GST-GAR was used as a substrate (*blue*), 4.5 μg of GST-GAR, 0.8 μg of GST-PRMT7, and 0.7 μM [^{3}H]AdoMet were incubated at 23 °C for 18 h. Product formation was analyzed as in *A* above; radioactivity in controls lacking enzyme (peptide assay) or enzyme and substrate (protein assay) were subtracted. *C*, metal ion effect. When H2B(23–37) was used as a substrate (*red bars*), the reactions containing 40 μM H2B(23–37), 0.4 μM GST-PRMT7, and 10 μM [^{14}C]AdoMet were incubated in the presence of 2 mM $MgCl_2$, $MgSO_4$, $CaCl_2$, or $ZnCl_2$ at 23 °C for 16 h. The positive control was performed in absence of metal ion; the negative control was performed in absence of enzyme and metal ion and was subtracted as background. When GST-GAR was used as a substrate (*blue bars*), the reactions containing 4.5 μg of GST-GAR, 0.8 μg of GST-PRMT7 and 0.7 μM [^{3}H]AdoMet were incubated in the presence of the indicated metal ions at 23 °C for 18 h. The negative control contained only [^{3}H]AdoMet and the buffer components and was subtracted as background. All measurements were performed in duplicate; *error bars* indicate the range.

activity dropped dramatically above 30 °C. These results were surprising for a mammalian enzyme presumably working at body temperatures of about 37 °C. To confirm this phenomenon, we also analyzed the temperature effect on the insect-expressed mouse PRMT7 (8) with H2B(23–37) as a substrate in the P81 paper assay (Fig. 9*B*) and the bacterially expressed human GST-PRMT7 with GST-GAR as a substrate in the fluorography assay (Fig. 9*C*). In both of these cases, a similar temperature dependence was found. These results indicate that PRMT7 is an unusual mammalian enzyme with significant activity at sub-physiological temperatures.

We also detected an unusual sensitivity of GST-PRMT7 to salt and the metal chelator EDTA. Using the peptide H2B(23–37), we found half-inhibition at about 30 mM NaCl (Fig. 10*A*). With the GST-GAR substrate, less salt sensitivity was seen, with a half-inhibition at about 180 mM NaCl. EDTA also showed an inhibitory effect on GST-PRMT7, with either the H2B(23–37) or GST-GAR substrate (Fig. 10*B*). At an EDTA concentration of 1 mM, enzyme activity was reduced by over 50% for both substrates. In experiments supplementing reaction mixtures with 2 mM $MgCl_2$, $MgSO_4$, $CaCl_2$, or $ZnCl_2$, we observed no increase in activity (Fig. 10*C*). The mechanism of inhibition of PRMT7 by EDTA remains to be established, although we note that zinc has been detected in the crystal structure of mouse PRMT7 (34).

DISCUSSION

We have confirmed the type III activity of bacterially expressed GST-tagged human PRMT7 on basic R*X*R sequence motifs under our optimized reaction conditions. Product formation was significantly improved as we adjusted several conditions from our previous study (7), particularly the reaction temperature. The type III activity of GST-PRMT7 forming only MMA product has been confirmed with both GST-GAR protein derived from fibrillarin and various peptides derived from histone H4, histone H2B, splicing protein SmD3, ribosomal protein RPL3, and HIV-1 TAT protein as well as for PRMT7 automethylation. These results are consistent with previous reports on human and mouse PRMT7 (7, 8) as well as studies on the trypanosome PRMT7 (6, 9). Although PRMT7 may work synergistically with type I or type II PRMTs or other modulators *in vivo*, PRMT7 by itself only generates MMA residues.

We find that effective substrates for GST-tagged human PRMT7 consist of sequences with at least two closely spaced arginine residues with adjacent basic residues. Out of all of the peptides tested (Table 1), H2B(23–27) bearing a KKRKRSRK sequence and P-TAT bearing an RKKRRQRRR sequence are the best PRMT7 substrates, probably because they contain a high density of positive charges and multiple arginine residues, which may be preferably recognized by the extra two acidic residues (Asp-147 and Glu-149) in the double E loop (Fig. 7). H4(1–21) bearing a KRHRK sequence, P-SmD3 bearing

RGRGK and RGRGR sequences, and P-RPL3 bearing an HRGLRK sequence are moderate substrates for PRMT7, suggesting the essential role of basic residue density. The H2B and H4 mutant peptides, where R*X*R sequences are modified to R*X*K or K*X*R sequences, are poor substrates. This demonstrates the importance of at least two arginine residues as the recognition site, which is also supported by the poor methylation of H4(1–8) and H3(1–7) sequences with a single arginine residue. These results are consistent with and extend those found earlier for the insect-expressed mouse enzyme (8).

Through site-directed mutagenesis, we show that the two additional acidic residues (Asp-147 and Glu-149) in the double E loop may be crucial elements in the substrate specificity of PRMT7 (Fig. 7). Enzymes where these residues are substituted with glycine and methionine, respectively, demonstrate dramatically decreased activity toward the H2B(23–37) and P-TAT substrates with high basic residue density but only moderately affected activity toward the P-SmD3 and GST-GAR substrates with relatively low basic residue density. It thus appears that the D147G and E149M mutations compromise the selectivity of PRMT7 for very basic R*X*R sites and that these two unique acidic residues in the PRMT7 double E loop are probably determinants for the preferable recognition of basic residues adjacent to or near the methylatable arginine residues.

We have also prepared PRMT7 with mutations in the double E loop designed to mimic conserved residues in type I and type II PRMTs (LFD to WMG and FD to LG, respectively). However, we found that neither of the mutated proteins displayed methyl transfer activity. Although the acidic residues do play an important role in conferring substrate specificity, mutating multiple residues in the double E loop destroys the ability of PRMT7 to methylate substrates. All of these mutations are within the catalytic N-terminal domain. PRMT7 also has an ancestrally duplicated C-terminal domain where many of the residues important for binding AdoMet or substrates have been altered. For example, only one of the glutamate residues in the corresponding region of the double E loop is present in the C-terminal domain (Glu-478). However, this domain is still required for enzyme activity (5), and in this study, we have shown that the E478Q mutation reduces the activity of PRMT7 to $<$1% of the wild-type activity. Although this second domain in PRMT7 is poorly conserved in sequence (5), it is certainly not redundant for substrate binding or catalysis.

In this study, we found special unique features of PRMT7 catalysis. First, the enzyme is more active at temperatures below the physiological mammalian value of 37 °C and in fact can perform catalysis even at 5 °C. Second, NaCl, EDTA, and some common metal ions were found to have a relatively strong inhibitory effect on PRMT7. These phenomena have not been observed for other members of the mammalian PRMT family. The unusual sensitivity to temperature may indicate that PRMT7 may be activated by cold stress to tissues.

Unfortunately, no *in vivo* substrates for PRMT7 have yet been unambiguously identified. Our results here, however, indicate that PRMT7-targeting sequences are often nucleotide binding sequences that compact and stabilize the structure of DNA/RNA, such as the HBR domain on histone H2B (28, 37), the RKKRRQRRR region (residues 49–57) on HIV-1 TAT protein (38), and the KRHRK region on histone H4 (39). The HBR domain at the end of the H2B N-terminal tail closely interacts with neighboring nucleosomal DNA and represses gene transcription (28, 37). In yeast, it was found that HBR is necessary and sufficient for repressing ~8.6% of genes, many of which are located near telomeres or involved in the metabolism of vitamins and carbohydrates (28). No *in vivo* evidence has been found for posttranslational modifications on the HBR domain, although *in vitro* data are very clear that insect-expressed mouse PRMT7 monomethylates Arg-29, Arg-31, and Arg-33 in this region (8). HIV-1 TAT residues 49–57 bear a nuclear localization signal and RNA-binding motif. This region has been reported to be asymmetrically dimethylated on Arg-52 and Arg-53 by PRMT6, leading to weaker interaction with the viral RNA and down-regulation of the transactivation capacity of TAT (40, 41). Our study suggests that arginine monomethylation may also occur in this region. Posttranslational modifications catalyzed by PRMT7 at these arginine and lysine-rich regions, although poorly characterized, may play an essential role in modulating their interactions with DNA/RNA. More efforts are needed to validate these possible methylation sites and the biological consequences of their modification *in vivo*.

Acknowledgments—We thank Paul Thompson and Heather Rust (Scripps Research Institute) for the kind gift of peptides H4(1–21), H4(1–21)R3K, and H4(1–21)R3MMA. We thank the previous and current members of the Clarke laboratory, in particular Alexander Patananan, Mingle Zhang, Kanishk Jain, Qais Al-Hadid, Cecilia Zurita-Lopez, and Jonathan Lowenson, for help.

REFERENCES

1. Bedford, M. T., and Clarke, S. G. (2009) Protein arginine methylation in mammals: who, what, and why. *Mol. Cell* **33,** 1–13
2. Herrmann, F., Pably, P., Eckerich, C., Bedford, M. T., and Fackelmayer, F. O. (2009) Human protein arginine methyltransferases *in vivo*: distinct properties of eight canonical members of the PRMT family. *J. Cell Sci.* **122,** 667–677
3. Yang, Y., and Bedford, M. T. (2013) Protein arginine methyltransferases and cancer. *Nat. Rev. Cancer* **13,** 37–50
4. Baldwin, R. M., Morettin, A., and Côté, J. (2014) Role of PRMTs in cancer: could minor isoforms be leaving a mark? *World J. Biol. Chem.* **5,** 115–129
5. Miranda, T. B., Miranda, M., Frankel, A., and Clarke, S. (2004) PRMT7 is a member of the protein arginine methyltransferase family with a distinct substrate specificity. *J. Biol. Chem.* **279,** 22902–22907
6. Fisk, J. C., Sayegh, J., Zurita-Lopez, C., Menon, S., Presnyak, V., Clarke, S. G., and Read, L. K. (2009) A type III protein arginine methyltransferase from the protozoan parasite *Trypanosoma brucei*. *J. Biol. Chem.* **284,** 11590–11600
7. Zurita-Lopez, C. I., Sandberg, T., Kelly, R., and Clarke, S. G. (2012) Human protein arginine methyltransferase 7 (PRMT7) is a type III enzyme forming ω-N^G-monomethylated arginine residues. *J. Biol. Chem.* **287,** 7859–7870
8. Feng, Y., Maity, R., Whitelegge, J. P., Hadjikyriacou, A., Li, Z., Zurita-Lopez, C., Al-Hadid, Q., Clark, A. T., Bedford, M. T., Masson, J. Y., and Clarke, S. G. (2013) Mammalian protein arginine methyltransferase 7 (PRMT7) specifically targets R*X*R sites in lysine- and arginine-rich regions. *J. Biol. Chem.* **288,** 37010–37025
9. Wang, C., Zhu, Y., Caceres, T. B., Liu, L., Peng, J., Wang, J., Chen, J., Chen, X., Zhang, Z., Zuo, X., Gong, Q., Teng, M., Hevel, J. M., Wu, J., and Shi, Y. (2014) Structural determinants for the strict monomethylation activity by *Trypanosoma brucei* protein arginine methyltransferase 7. *Structure* **22,** 756–768

10. Kim, C., Lim, Y., Yoo, B. C., Won, N. H., Kim, S., and Kim, G. (2010) Regulation of post-translational protein arginine methylation during HeLa cell cycle. *Biochim. Biophys. Acta* **1800,** 977–985
11. Lu, H., Cui, J. Y., Gunewardena, S., Yoo, B., Zhong, X. B., and Klaassen, C. D. (2012) Hepatic ontogeny and tissue distribution of mRNAs of epigenetic modifiers in mice using RNA-sequencing. *Epigenetics* **7,** 914–929
12. Buhr, N., Carapito, C., Schaeffer, C., Kieffer, E., Van Dorsselaer, A., and Viville, S. (2008) Nuclear proteome analysis of undifferentiated mouse embryonic stem and germ cells. *Electrophoresis* **29,** 2381–2390
13. Dhar, S. S., Lee, S. H., Kan, P. Y., Voigt, P., Ma, L., Shi, X., Reinberg, D., and Lee, M. G. (2012) Trans-tail regulation of MLL4-catalyzed H3K4 methylation by H4R3 symmetric dimethylation is mediated by a tandem PHD of MLL4. *Genes Dev.* **26,** 2749–2762
14. Baldwin, E. L., and Osheroff, N. (2005) Etoposide, topoisomerase II and cancer. *Curr. Med. Chem. Anticancer Agents* **5,** 363–372
15. Bleibel, W. K., Duan, S., Huang, R. S., Kistner, E. O., Shukla, S. J., Wu, X., Badner, J. A., and Dolan, M. E. (2009) Identification of genomic regions contributing to etoposide-induced cytotoxicity. *Hum. Genet.* **125,** 173–180
16. Verbiest, V., Montaudon, D., Tautu, M. T., Moukarzel, J., Portail, J. P., Markovits, J., Robert, J., Ichas, F., and Pourquier, P. (2008) Protein arginine (*N*)-methyl transferase 7 (PRMT7) as a potential target for the sensitization of tumor cells to camptothecins. *FEBS Lett.* **582,** 1483–1489
17. Gros, L., Delaporte, C., Frey, S., Decesse, J., de Saint-Vincent, B. R., Cavarec, L., Dubart, A., Gudkov, A. V., and Jacquemin-Sablon, A. (2003) Identification of new drug sensitivity genes using genetic suppressor elements: protein arginine n-methyltransferase mediates cell sensitivity to DNA-damaging agents. *Cancer Res.* **63,** 164–171
18. Gros, L., Renodon-Cornière, A., de Saint Vincent, B. R., Feder, M., Bujnicki, J. M., and Jacquemin-Sablon, A. (2006) Characterization of prmt7α and β isozymes from Chinese hamster cells sensitive and resistant to topoisomerase II inhibitors. *Biochim. Biophys. Acta* **1760,** 1646–1656
19. Jelinic, P., Stehle, J. C., and Shaw, P. (2006) The testis-specific factor CTCFL cooperates with the protein methyltransferase PRMT7 in H19 imprinting control region methylation. *PLoS Biol.* **4,** e355
20. Gonsalvez, G. B., Tian, L., Ospina, J. K., Boisvert, F. M., Lamond, A. I., and Matera, A. G. (2007) Two distinct arginine methyltransferases are required for biogenesis of Sm-class ribonucleoproteins. *J. Cell Biol.* **178,** 733–740
21. Thomassen, M., Tan, Q., Kruse, T. A. (2009) Gene expression meta-analysis identifies chromosomal regions and candidate genes involved in breast cancer metastasis. *Breast Cancer Res. Treat.* **113,** 239–249
22. Yao, R., Jiang, H., Ma, Y., Wang, L., Wang, L., Du, J., Hou, P., Gao, Y., Zhao, L., Wang, G., Zhang, Y., Liu, D. X., Huang, B., and Lu, J. (2014) PRMT7 induces epithelial-to-mesenchymal transition and promotes metastasis in breast cancer. *Cancer Res.* **74,** 5656–5667
23. Osborne, T. C., Obianyo, O., Zhang, X., Cheng, X., and Thompson, P. R. (2007) Protein arginine methyltransferase 1: positively charged residues in substrate peptides distal to the site of methylation are important for substrate binding and catalysis. *Biochemistry* **46,** 13370–13381
24. Obianyo, O., Osborne, T. C., and Thompson, P. R. (2008) Kinetic mechanism of protein arginine methyltransferase 1. *Biochemistry* **47,** 10420–10427
25. Lee, J. H., Cook, J. R., Yang, Z. H., Mirochnitchenko, O., Gunderson, S. I., Felix, A. M., Herth, N., Hoffmann, R., and Pestka, S. (2005) PRMT7, a new protein arginine methyltransferase that synthesizes symmetric dimethylarginine. *J. Biol. Chem.* **280,** 3656–3664
26. Feng, Y., Wang, J., Asher, S., Hoang, L., Guardiani, C., Ivanov, I., and Zheng, Y. G. (2011) Histone H4 acetylation differentially modulates arginine methylation by an in *cis* mechanism. *J. Biol. Chem.* **286,** 20323–20334
27. Gary, J. D., and Clarke, S. (1998) RNA and protein interactions modulated by protein arginine methylation. *Prog. Nucleic Acid Res. Mol. Biol.* **61,** 65–131
28. Parra, M. A., Kerr, D., Fahy, D., Pouchnik, D. J., and Wyrick, J. J. (2006) Deciphering the roles of the histone H2B N-terminal domain in genome-wide transcription. *Mol. Cell Biol.* **26,** 3842–3852
29. Feng, Y., Xie, N., Jin, M., Stahley, M. R., Stivers, J. T., and Zheng, Y. G. (2011) A transient kinetic analysis of PRMT1 catalysis. *Biochemistry* **50,** 7033–7044
30. Antonysamy, S., Bonday, Z., Campbell, R. M., Doyle, B., Druzina, Z., Gheyi, T., Han, B., Jungheim, L. N., Qian, Y., Rauch, C., Russell, M., Sauder, J. M., Wasserman, S. R., Weichert, K., Willard, F. S., Zhang, A., and Emtage, S. (2012) Crystal structure of the human PRMT5:MEP50 complex. *Proc. Natl. Acad. Sci. U.S.A.* **109,** 17960–17965
31. Strahl, B. D., Briggs, S. D., Brame, C. J., Caldwell, J. A., Koh, S. S., Ma, H., Cook, R. G., Shabanowitz, J., Hunt, D. F., Stallcup, M. R., and Allis, C. D. (2001) Methylation of histone H4 at arginine 3 occurs *in vivo* and is mediated by the nuclear receptor coactivator PRMT1. *Curr. Biol.* **11,** 996–1000
32. Pal, S., Baiocchi, R. A., Byrd, J. C., Grever, M. R., Jacob, S. T., and Sif, S. (2007) Low levels of miR-92b/96 induce PRMT5 translation and H3R8/H4R3 methylation in mantle cell lymphoma. *EMBO J.* **26,** 3558–3569
33. Zhang, X., and Cheng, X. (2003) Structure of the predominant protein arginine methyltransferase PRMT1 and analysis of its binding to substrate peptides. *Structure* **11,** 509–520
34. Cura, V., Troffer-Charlier, N., Wurtz, J. M., Bonnefond, L., and Cavarelli, J. (2014) Structural insight into arginine methylation by the mouse protein arginine methyltransferase 7: a zinc finger freezes the mimic of the dimeric state into a single active site. *Acta Crystallogr. D Biol. Crystallogr.* **70,** 2401–2412
35. Hasegawa, M., Toma-Fukai, S., Kim, J. D., Fukamizu, A., and Shimizu, T. (2014) Protein arginine methyltransferase 7 has a novel homodimer-like structure formed by tandem repeats. *FEBS Lett.* **588,** 1942–1948
36. Tang, J., Gary, J. D., Clarke, S., and Herschman, H. R. (1998) PRMT3, a type I protein arginine *N*-methyltransferase that differs from PRMT1 in its oligomerization, subcellular localization, substrate specificity, and regulation. *J. Biol. Chem.* **273,** 16935–16945
37. Wyrick, J. J., and Parra, M. A. (2009) The role of histone H2A and H2B post-translational modifications in transcription: a genomic perspective. *Biochim. Biophys. Acta* **1789,** 37–44
38. Truant, R., and Cullen, B. R. (1999) The arginine-rich domains present in human immunodeficiency virus type 1 Tat and Rev function as direct importin β-dependent nuclear localization signals. *Mol. Cell Biol.* **19,** 1210–1217
39. Ebralidse, K. K., Grachev, S. A., and Mirzabekov, A. D. (1988) A highly basic histone H4 domain bound to the sharply bent region of nucleosomal DNA. *Nature* **331,** 365–367
40. Boulanger, M. C., Liang, C., Russell, R. S., Lin, R., Bedford, M. T., Wainberg, M. A., and Richard, S. (2005) Methylation of Tat by PRMT6 regulates human immunodeficiency virus type 1 gene expression. *J. Virol.* **79,** 124–131
41. Xie, B., Invernizzi, C. F., Richard, S., and Wainberg, M. A. (2007) Arginine methylation of the human immunodeficiency virus type 1 Tat protein by PRMT6 negatively affects Tat interactions with both cyclin T1 and the Tat transactivation region. *J. Virol.* **81,** 4226–4234